Optical properties of arrays of quantum dots with internal disorder

E. V. Tsiper
*Department of Physics, University of Utah, Salt Lake City, Utah 84112**

arXiv:cond-mat/9508149v1 1 Sep 1995

Optical properties of large arrays of isolated quantum dots are discussed in order to interpret the existent photoluminescence data. The presented theory explains the large observed shift between the lowest emission and absorption energies as the average distance between the ground and first excited states of the dots. The lineshape of the spectra is calculated for the case when the fluctuations of the energy levels in quantum dots are due to the alloy composition fluctuations. The calculated lineshape is in good agreement with the experimental data. The influence of fluctuations of the shape of quantum dots on the photoluminescence spectra is also discussed.

I. INTRODUCTION

Reduced-dimensionality structures are currently attracting much attention.[1–4] Modern technology made it possible to create nanoscale 0D structures where motion in all directions is quantized (quantum dots). Often a system represents a large array of independent quantum dots. Because of extremely small dimensions, the fluctuations of parameters of individual quantum dots become an important factor since they determine the properties of the whole array.

This paper was initiated by the experimental work Ref. 1, where nice photoluminescence (PL) and photoluminescence excitation (PLE) experiments were performed with an array of self-assembling quantum dots. The conventional nonselective (with above-barrier excitation) PL reveals a broad peak of about ~ 50 meV in width. This width originates from a wide spread of energies of different quantum dots in the array. Both PLE and selectively-excited PL spectra (when only the quantum dots that are in resonance with incident light are excited) show sets of broadened peaks with 2-3 times smaller widths. These peaks correspond to the distribution of energy levels in the subset of quantum dots that are resonantly excited. It was observed that the first PLE peak is strongly shifted from the detection energy. The origin of this shift remained unclear. Moreover, no measurable Stokes shift was observed in a recent paper Ref. 3, where the PL has been measured together with the direct absorption by the layer of quantum dots.

In this paper a simple theory of the PL from an array of quantum dots is developed. We suggest that the process of photoexcitation of a dot into its lowest optically-excited state does not contribute to the PL signal. The proposed interpretation of the experimental data explains large Stokes-like shift between the PL and PLE peaks as the average distance between the two lowest optically-excited states. In what follows we use the term "ground state" to denote the lowest optically-excited state because it corresponds to the ground state of the photoexcited carriers in the dot.

It is suggested that the PL and PLE lineshapes are completely determined by the statistical distribution of the energy levels of different quantum dots in the array. More precisely, it is determined by the distribution of *pairs* of energy levels. It is shown that such distribution is essentially two-variable. That is, there exists a correlation in the positions of different energy levels in each quantum dot throughout the array, however, such correlation is not 100%. We show that this feature causes the difference in the positions of the maxima of the PL and PLE spectra.

The fluctuations of energy levels due to the random potential caused by the alloy composition fluctuations are studied in Section IV. We show that the major part of the observed linewidth can be accounted for by this mechanism. We also suggest that the first two excited states observed in Ref. 1 originate from the twofold degenerate first excited level, when the degeneracy is lifted by the random potential. The density of states and the two-level distribution function, which accounts for the correlation in energy-level positions, are calculated. The spectra determined by these functions describe most of the features of the experimental spectra.

Finally, the effects caused by fluctuations of the *shape* of the quantum dots are discussed. It is suggested that the fluctuations of the shape of the dots should increase the energy-level correlation.

II. ORIGIN OF THE STOKES-LIKE SHIFT

In the present paper we consider the case when both the electron and the hole are confined in the quantum dot. Energy of the quantum dot is measured from the unexcited state of the dot with no electrons and holes. The term "ground state" refers to the ground state of the quantum dot with an excited electron-hole pair, i.e. to the lowest optically-excited state.

The key feature of an array of quantum dots that differs it from a quantum well or bulk material is that there is no charge transfer between the dots, or at least such transfer is strongly suppressed. Different quantum dots therefore give independent additive contributions in any optical experiment.[5]

The density of states for each quantum dot represents a set of delta-function-like peaks, while the total density of states of the whole system can be spread in a wide energy range due to the inhomogeneous broadening. Several experiments have been reported recently where the contributions to the luminescence from *single* quantum dots were found.[2–4,6] Single quantum dots give extremely narrow sub-meV spectral lines. When, however, the number of the excited quantum dots is large, a broad luminescence peak is observed.[1,3,4]

We suggest that such a feature makes it difficult to probe optically the ground states of the dots and thus causes an apparent Stokes-like shift observed in Ref. 1. Probing of the ground states of the dots may require special technique like high resolution or time-resolved PL.

Indeed, let's consider the contribution to the PL from the process when the photon is absorbed into the ground state of a dot and then re-emitted. If the optical process is not phonon-assisted, the energies of the incoming and outgoing photons are exactly equal. The PL response can hardly be observed since it is hidden by the incident beam scattered by other elements of the experimental environment. This situation is quite different from that in quantum wells or bulk semiconductors, where an electron excited to the conduction band has always quantum states with smaller energies. It can loose some energy before it recombines in an *independent* optical process.

In a quantum dot, the emitted photon may have its energy below (or above) that of the exciting light if the PL is phonon-assisted. However, the phonon must be emitted (absorbed) together with photon *in the same quantum process*. The probability of such process is determined in higher-order perturbation theory in the electron-phonon coupling constant and is therefore much smaller than the probability of the direct transition.

In order to give a substantial contribution to the PL signal, the dot must be pumped into one of its *excited* states. Therefore, the minimum distance between the excitation and detection energies seen in the spectra is equal to the distance between the ground and first excited states of the dot. In fact, no Stokes shift was found between the PL and the direct absorption by a layer of quantum dots measured in Ref. 3.

III. POSITIONS OF PEAKS IN THE PL AND PLE SPECTRA

In this section the shape of the PL and PLE spectra is described qualitatively. Different peaks observed in the spectra are assigned. It is shown that existence of a random spread of interlevel distances in quantum dots causes substantial deviations of the positions of peaks seen in PLE and selectively-excited PL spectra.

We shall assume for simplicity that the energy relaxation in a quantum dot occurs faster than recombination, so that the light is always emitted from the ground state of the dot.

Let us first consider a simple model when the distances between different energy levels are the same for all quantum dots, however, there is a wide distribution of energy levels in the array. In other words, let the picture of energy levels be the same in each quantum dot but shifted randomly as a whole. This implies a 100% correlation in the positions of different energy levels in each dot.

If the conventional PL technique is used so that the pumping is performed with energies well above the barriers between the dots, all the dots are excited and emit light at their ground-state energies. The emission then represents a broad peak due to the wide distribution of the ground-state energies.

Let us now consider PLE and selectively-excited PL measurements. Here only those dots are excited, which have one of their energy levels in resonance with the exciting light. As suggested above, the dots pumped into their ground states do not contribute to the spectra. When the interlevel distances are the same in all dots, both PLE and selectively-excited PL spectra would show a set of delta-function-like peaks as sketched in the Fig. 1.

It is more convenient to start with the PLE (left). By fixing the detection energy one selects the subset of all quantum dots in the array with the ground-state energy $E_0 = E_{detector}$ (we have assumed that the light is always emitted from the ground state of the dots). The PLE signal appears when the excitation energy matches the energy of an excited state ($E_{laser} = E_1$, E_2, etc.) in the selected subset. Thus the first observed (lowest in energy) PLE peak corresponds to the *first excited energy levels of such dots* that have their ground-state level at the detection energy.

The analysis of the selectively-excited PL (right) is somewhat more complicated but similar. The fixed energy of excitation selects *several* subsets of all quantum dots such that $E_1 = E_{laser}$, $E_2 = E_{laser}$, etc. A nonzero PL signal appears when the detection energy matches the ground-state energy of one of the subsets. The position of the first observed PL peak (highest in energy) thus corresponds to the *ground state energy of such dots* that have their *first excited* energy level at the excitation energy. The distance between the first two PL peaks is equal to E_{21}, the distance between *the first and the second* excited states of the dots.

When interlevel distances are the same in all dots, all distances between different peaks in the PL (PLE) series also remain the same, while the whole picture shifts with the shift of the laser (detector) energies. It means that positions of these peaks being plotted against the laser (detector) energies must form a set of straight lines with the unit slope.

The slopes of such lines obtained from the PLE and selectively-excited PL spectra obtained in Ref. 1 are all less then 1. For the first PL and PLE peaks, e.g., $dE^{PL}_{max,1}/dE_{laser} = 0.91$, $dE^{PLE}_{max,1}/dE_{detector} = 0.77$.[1]

It is easy to see that such deviation cannot be attributed to the dependence of the interlevel distances on the ground-state energy. Indeed, in this case the slopes

obtained from the PL and PLE spectra should be inverse of each other. We see, however, that

$$\frac{dE^{PL}_{max,m}}{dE_{laser}} \neq \left(\frac{dE^{PLE}_{max,m}}{dE_{detector}} \right)^{-1} . \quad (1)$$

We show below that existence of a spread of interlevel distances in the array causes deviation of the positions of peaks seen in the PL and PLE spectra in such a way that both derivatives in Eq. (1) become less then 1.

To demonstrate this, let us assume that the interlevel distances in the dots fluctuate randomly in some (narrow) energy interval. In this case selection of a subset of quantum dots by fixing one of the energy levels does not yet determine the positions of other energy levels. Then one should observe a sequence of broadened peaks in both PL and PLE. The scale of broadening is determined by the distribution of interlevel distances only, therefore it can be narrower than the distribution of the absolute energies. As shown below such behavior is natural if the spread is caused by a random potential.

To understand how the *positions of maxima of the broadened peaks* are shifted, it is convenient to draw a three-dimensional picture shown in Fig. 2. Here the intensity measured by the detector is plotted as a function of two variables — the excitation and the emission energies. Clearly, such a plot contains all information, which both PL and PLE can provide. To get the shapes of the PL or PLE spectra one simply has to slice the three-dimensional plot along the E_{laser} or $E_{detector}$ axis.

First, the intensity is zero in the half-plane $E_{laser} < E_{detector}$. The intensity is nonzero only when E_{laser} and $E_{detector}$ are in resonance with the excited and ground states of some dot *simultaneously*. If the spread of interlevel distances is small, the three-dimensional plot has a shape of a set of narrow *ridges*, elongated in the direction parallel to the line $E_{laser} = E_{detector}$. Each ridge corresponds to the optical process for which $E_{detector} = E_0$ and $E_{laser} = E_m$, m=1, 2, etc. The width of each ridge is determined by the spread of the corresponding interlevel distances, while the length is larger and represents the large spread of the ground-state energies. The distance between the ridge and the line $E_{laser} = E_{detector}$ is determined by the average distance between the ground and the corresponding excited states of the dots.

The inset in Fig. 2 shows a fragment of the same plot in the isoline projection (dashed lines). Crosses and pluses show the positions of the maxima in the PL and PLE crossections respectively. The "PL and PLE lines" are the loci of the maxima observed in the PL and PLE spectra.

As one can see, the positions of the maxima deviate from the major axis of the ridge and from each other. Indeed, these positions lie in such points where the crossection line (parallel to one of the axes) is tangential to the lines of equal intensity. Note that the deviation of the positions of the maxima is such that both derivatives in the Eq. (1) are less than 1.

Both lines intersect exactly at the maximum of the ridge, which coordinates give the average positions of the ground and the excited states of all the dots in the array.

In general, if the oscillator strengths are the same for all allowed transitions, the intensity as a function of the excitation and detection energies is proportional to the mutual level-level distribution function: $I(E_{detector}, E_{laser}) \propto \sum_m P(E_{detector} = E_0, E_{laser} = E_m)$, where E_m are the energy-level positions, E_0 being the position of the ground state. In the following section we derive the shape of the distribution function $P(E_0, E_m)$ when the spread of the energy-level positions is caused by the composition fluctuations. We show that a quite complicated PL and PLE lineshape observed in Ref. 1 can be sufficiently well described in this way.

IV. FLUCTUATIONS OF ENERGY LEVELS IN QUANTUM DOTS

In this section we study the properties of the statistical distribution of the energy levels in quantum dots caused by a white-noise random potential. We present a strong evidence that the major part of the observed spread of the PL and PLE peaks is caused by universal composition fluctuations in the dots. These fluctuations are a generic property of semiconductor alloys and produce a theoretical limit for unification of quantum dots in an array.

We also suggest that the first two excited levels that reveal themselves in the PLE and selectively-excited PL experiments originate *from a single doubly degenerate level* when the degeneracy is lifted by the random potential.

In semiconductor alloys the lattice sites are occupied randomly with two types of substitutional atoms. We ignore here the correlation between occupation of different sites. The composition x averaged over a small volume always fluctuates. The order of magnitude of the fluctuations is inversely proportional to the square root of the volume over which the averaging is performed. Though usually small, this effect can be important in extremely small structures.

In small quantum dots such composition fluctuations cause shifts of energy levels from the positions determined by the average composition x_0. The "local" composition x varies from dot to dot, and also *inside* the dot. According to that, the energy levels fluctuate from dot to dot. Shifts of the energy levels in different quantum dots are independent from each other. Inside a single quantum dot the shifts of different energy levels are correlated. Note, however, that such correlation is not 100% (as it would be if there was only one fluctuating parameter like the diameter of a dot).

In order to calculate the statistical distribution of energy levels caused by composition fluctuations we use the method developed by Efros and Raikh (for a review see Ref. 7). This method is applicable if the size of the wave

function is much larger than the lattice constant. In this case one needs to know only the shape of the wave function in a quantum dot and the slope of the dependence of the gap on composition, dE_g/dx, at average composition x_0.

The result depends on whether the unperturbed energy levels are degenerate or not. Without degeneracy the distribution of energy levels E_m is Gaussian with the standard deviation given by

$$\sigma_m^2 = \overline{\epsilon_m^2} = \gamma \int d^3r \ \psi_m^4(\mathbf{r}), \tag{2}$$

where $\epsilon_m = E_m - \overline{E}_m$, ψ_m is the wave function (real) corresponding to the energy level E_m, and γ is given by

$$\gamma = \left(\frac{dE_g}{dx}\right)^2 \frac{x_0(1-x_0)}{N}, \tag{3}$$

where N is the number of lattice sites per unit volume.

The *covariance* between ϵ_m and ϵ_n can be obtained in a similar way:

$$\overline{\epsilon_m \epsilon_n} = \rho \sigma_m \sigma_n = \gamma \int d^3r \ \psi_m^2(\mathbf{r}) \psi_n^2(\mathbf{r}). \tag{4}$$

The coefficient ρ, $\rho \leq 1$, is called the coefficient of correlation between E_m and E_n.

To find the shape of the PLE and selectively-excited PL spectra we need the mutual distribution function for E_0 and E_m. The most general form of the two-variable Gaussian distribution is given by

$$G_2(\epsilon_0, \epsilon_m; \sigma_0, \sigma_m, \rho) = \frac{1}{2\pi\sigma_0\sigma_m\sqrt{1-\rho^2}} \times \exp\left\{-\frac{1}{2(1-\rho^2)}\left[\frac{\epsilon_0^2}{\sigma_0^2} - 2\rho\frac{\epsilon_0\epsilon_m}{\sigma_0\sigma_m} + \frac{\epsilon_m^2}{\sigma_m^2}\right]\right\}, \tag{5}$$

This is just an analytical expression for the shape of the ridge, discussed in the previous section. The ridge is strongly elongated when the parameter ρ is close to 1. It is equal to 1 in the limiting case when an exact relation between the energy-level positions exists, so that the two-variable statistical distribution becomes effectively one-variable. The ratio σ_m/σ_0 determines the orientation of the ridge. The ridge is parallel to the line $E_{laser} = E_{detector}$ when $\sigma_m = \sigma_0$.

The situation is, however, more complicated if a degeneracy exists. The random potential shifts the degenerate energy level and lifts the degeneracy. The distribution of energies in the vicinity of an unperturbed degenerate level appears to be not Gaussian. The mutual two-variable distribution function for a transition between E_0 and E_m is not Gaussian either. Instead, it has a shape of two close parallel ridges corresponding to each of the split-off energy levels.

For simplicity we restrict ourselves to the axially symmetric quantum dots, where each energy level except the ground state is doubly degenerate. In this case it appears to be possible to derive the general form of the distribution function without knowledge of the shape of the wave functions in the quantum dot.

For an axially symmetric system two degenerate wave functions with the angular momentum $|m|$ have the form $\psi_{m\pm}(\mathbf{r}) = \psi_m(r)e^{\pm im\phi}$, where ψ_m can be made real. The positions of energy levels $E_{m\pm}$, split and shifted by random potential of the particular configuration, can be obtained as the eigenvalues of the secular matrix

$$\delta H = \begin{bmatrix} u & x+iy \\ x-iy & u \end{bmatrix}, \tag{6}$$

where the matrix elements u and $x+iy$ take random values in each quantum dot and are given by:

$$u = \sqrt{\gamma} \int d^3r \ V(\mathbf{r})\psi_m^2(\mathbf{r}), \tag{7a}$$

$$x + iy = \sqrt{\gamma} \int d^3r \ V(\mathbf{r})\psi_m^2(\mathbf{r})e^{2im\phi}. \tag{7b}$$

Here $V(\mathbf{r})$ is the white-noise random potential with correlator $< V(\mathbf{r})V(\mathbf{r}') >= \gamma\delta(\mathbf{r}-\mathbf{r}')$.

Eigenvalues of δH are $\epsilon_\pm = u \pm \sqrt{x^2+y^2}$ (the energy is measured from the unperturbed energy level). It is easy to see that u, x, and y are *independent* Gaussian random variables with $\overline{u^2} = \sigma_m^2$, $\overline{x^2} = \overline{y^2} = \sigma_m^2/2$, σ_m^2 being given by Eq. (2).

The density of states in the vicinity of E_m (the distribution function for $\epsilon_m = E_m - \overline{E}_m$) is given by

$$\begin{aligned} P(\epsilon_m) &= \sum_{\pm} \int\int\int du dx dy \ \delta(\epsilon_m - u \mp \sqrt{x^2+y^2}) \\ &\quad \times G_1(u;\sigma_m) G_1(x;\frac{\sigma_m}{\sqrt{2}}) G_1(y;\frac{\sigma_m}{\sqrt{2}}) \\ &= D_0(\epsilon_m;\sigma_m), \end{aligned} \tag{8}$$

where G_1 is the standard one-variable Gaussian distribution, $G_1(\epsilon;\sigma) \equiv \sigma^{-1}G_1(\epsilon/\sigma;1)$, $G_1(z;1) = (2\pi)^{-1/2} \times \exp(-z^2/2)$; and we have introduced the notation for the distribution function $D_0(\epsilon;\sigma) \equiv \sigma^{-1}D_0(\epsilon/\sigma;1)$,

$$D_0(z;1) = \frac{2}{3}\sqrt{\frac{2}{\pi}}e^{-z^2/2} + \frac{2z}{3\sqrt{3}}e^{-z^2/3}\mathrm{erf}(\frac{z}{\sqrt{6}}). \tag{9}$$

The meaning of the index 0 in $D_0(\epsilon;\sigma)$ will soon become clear.

The Eq. (9) describes a bell-shaped curve, which determines the density of states and, hence, the *absorption spectrum* in the vicinity of the excited level E_m. It's shape can be fairly well approximated by a Gaussian with the effective dispersion $\sigma_{eff} = \sigma_m\sqrt{2}$, as shown in Fig. 3.

In order to find the mutual two-level distribution function that determines the shape of the PL and PLE spectra it is important to account for the correlation between

matrix elements of δH and the shift of the ground-state ϵ_0.

It is useful to note that the expression for the matrix element u is the same as the expression for the shift of a non-degenerate level with the wave function $\psi_m(r)$. The value of u is, therefore, *correlated* with ϵ_0 via the same two-variable Gaussian distribution as in Eq. (5): $P(\epsilon_0, u) = G_2(\epsilon_0, u; \sigma_0, \sigma_m, \rho)$, with the parameters σ_0, σ_m, and ρ given by Eqs. (2), (4). The parameters x and y are statistically independent of ϵ_0 and u, because the corresponding covariances become zero when the integration over the azimuthal angle ϕ is performed. Thus, we obtain:

$$P(\epsilon_0, \epsilon_m) = \sum_{\pm} \int\int\int du dx dy \; \delta(\epsilon_m - u \mp \sqrt{x^2+y^2}) \times G_2(\epsilon_0, u; \sigma_0, \sigma_m, \rho) G_1(x; \frac{\sigma_m}{\sqrt{2}}) G_1(y; \frac{\sigma_m}{\sqrt{2}}) = G_1(\epsilon_0; \sigma_0) D_\rho(\epsilon_m - \epsilon_0 \rho \frac{\sigma_m}{\sigma_0}; \sigma_m), \qquad (10)$$

where the function $D_\rho(\epsilon; \sigma) \equiv \sigma^{-1} D_\rho(\epsilon/\sigma; 1)$, and

$$D_\rho(z; 1) = \frac{2\sqrt{\mu - 1}}{\sqrt{\pi}\mu} \exp\left(-\frac{z^2}{\mu - 1}\right) + \frac{2z}{\mu^{3/2}} \exp\left(-\frac{z^2}{\mu}\right) \mathrm{erf}\left[\frac{z}{\sqrt{\mu(\mu-1)}}\right]. \qquad (11)$$

Here $\mu = 3 - 2\rho^2$. The function $D_0(\epsilon; \sigma)$ defined by Eq. (9) is a particular case of (11) with $\rho = 0$.

The function $D_\rho(\epsilon_m; \sigma_m)$ gives the distribution of the energy sublevels in the vicinity of $\overline{E}_m$, when *the position of the ground state is fixed*. It is normalized in such a way that $\int d\epsilon \; D_\rho(\epsilon; \sigma) = 2$ (according to the twofold degeneracy), and $\int d\epsilon \; \epsilon^2 D_\rho(\epsilon; \sigma) = 2\sigma^2(2 - \rho^2)$. The function $D_\rho(\epsilon; \sigma)$ is symmetric in ϵ. It has one maximum when $\rho \leq 1/\sqrt{2}$ and two maxima, when $\rho > 1/\sqrt{2}$. The maxima become more pronounced when ρ tends to 1.

The function $P(\epsilon_0, \epsilon_m)$ determined by Eq. (10) gives the probability density for a quantum dot to have the ground state at the energy $\overline{E}_0 + \epsilon_0$ and an excited state at the energy $\overline{E}_m + \epsilon_m$. It is proportional to the intensity measured by the detector at fixed excitation and detection energies. Hence, it determines the shape of both PL and PLE spectra when the proper argument is fixed.

The function $P(\epsilon_0, \epsilon_m)$ appears to be not very sensitive to the ratio σ_m/σ_0. It is, however, quite sensitive to the value of the correlation coefficient ρ. This function is plotted in Fig. 4 for $\sigma_m = \sigma_0$ and two different values of ρ. As shown in the next section, it is natural for the coefficient ρ to be close to 1. The value $\rho = 0.94$ [Fig. 4(a)] gives the best fit to the experimental data. When ρ tends to 1 [Fig. 4(b)] the intensity in the dip between two maxima approaches zero. The lineshapes of the spectra described by Eq. (10) are discussed in detail in the next section.

V. DISCUSSION

We replot the positions of the PL and PLE maxima observed in Ref. 1 on the combined plot in Fig. 5 to illustrate that the experimental behavior is in agreement with our consideration (compare with the inset in Fig. 2). The dotted line shows unit slope, $E_{laser} = E_{detector}$. Three lines correspond to the positions of two maxima observed in each PL curve (crosses) and one — in each PLE curve (pluses). Positions of only one PLE maximum for each $E_{detector}$ are shown because the second PLE maximum is seen not clear enough. The constant value of 1290 meV has been subtracted from all energies.

Three lines shown in Fig. 5 are consistent with the qualitative picture of two close parallel ridges. As suggested above, these ridges correspond to the two optical processes where $E_{detector} = E_0$ and $E_{laser} = E_{1\pm}$; E_0 being the ground-state energy and $E_{1\pm}$ — the energies of the first and second excited states.

We use the notation $E_{1\pm}$ instead of $E_{1,2}$ for the two excited states according to the idea that they originate from the twofold-degenerate first excited energy level E_1 when the degeneracy is lifted by random potential. This idea is supported by the fact that the ratio of interlevel distances appears to be $(\overline{E}_{1+} - \overline{E}_{1-})/(\overline{E}_{1-} - \overline{E}_0) \approx 0.6$. For a cylindrical quantum well with infinite potential walls the corresponding ratio is about $(\overline{E}_{21}/\overline{E}_{10}) = 1.3$.

The point of intersection of two lines gives the position of the maximum of the first ridge. The difference of 55 meV in its coordinates is nothing but the observed Stokes-like shift between emission and absorption energies. The distance between two ridges measured along the E_{laser} axis gives $\overline{E}_{1+} - \overline{E}_{1-}$, the mean splitting of the excited state E_1.

Using Fig. 5 we may conclude that the average distance between the ground and (split) first excited state is about 75 meV, while the average splitting of the excited state is approximately 40 meV.

Fig. 6 shows the comparison between the presented theory and the experiment. The experimental spectra from Ref. 1 are replotted in Fig. 6(a). The theoretical PLE and selectively-excited PL spectra [Fig. 6(b)] are obtained with the use of Eq. (10) by fixing ϵ_0 or ϵ_m respectively. Experimental values for the average positions of the energy levels $\overline{E}_0 = 1276$ meV and $\overline{E}_1 = 1351$ meV are used.

The Fig. 6(b) is essentially the Fig. 4(a), replotted in the wavelength scale for better comparison. The value $\rho = 0.94$ gives the best fit for the data from Ref. 1. It is seen that the curves obtained reproduce all the features of both PL and PLE spectra.

The structure of the expression (10) is such that if ϵ_0 is fixed, it describes a curve symmetric around the point $\epsilon_m = \epsilon_0 \rho \sigma_m/\sigma_0$. Thus (if $\rho > 1/\sqrt{2}$) the PLE line should reveal two *symmetric* peaks at any detection energy. This is exactly the behavior seen in the experiment. When the detection energy is changed, the whole spectrum must

shift linearly with it. Indeed, Fig. 5 shows that the positions of PLE maxima depend linearly on the detection energy. The slope of the PLE curve in Fig. 5 gives the ratio σ_1/σ_0, which appears to be close to 1.

If the position of the excited level, ϵ_m, is fixed, the lineshape is asymmetric. When ρ is close to 1, the PL lineshape also shows two maxima, however, there is a peculiar interplay in their magnitudes when the excitation energy is changed. This also matches the experimental data quite well.

Such interplay can be easily understood. First (second) PL maximum corresponds to the distribution of ground-state energies of such subset of quantum dots, for which the lowest (highest) split-off level coincides with E_{laser}. When E_{laser} is below $\overline{E}_m$, the amounts of first type of dots is larger than that of the second type. When E_{laser} is larger than $\overline{E}_m$, the dots of the second type win.

The interplay is absent in PLE, because for each fixed ground-state energy there is always equal amount of lowest and highest split-off levels.

The magnitudes of σ_1 and σ_0 can be obtained independently as follows. For $\rho = 0.94$, the maximum of $D_\rho(\epsilon;\sigma)$ lies at $\epsilon = 0.765\sigma$. Then, from the position of the PLE maximum, σ_1=14.5 meV/0.765=19 meV. The spread of the ground states σ_0 can be determined independently from the nonselective PL [curve 9 in Fig. 6(a)]. It gives σ_0=18.2 meV.

If we know the shape of the wave function, we may find the values for the parameters $\sigma_{0,1}$ and ρ, using Eqs. (2,4). As a guess, we may try the wave functions for the cylindrical quantum well with infinite walls:

$$\psi_m(\mathbf{r}) \propto \cos(\frac{\pi r_\perp}{h}) J_m(\frac{\nu_m r_\parallel}{R}), \qquad (12)$$

where h and R are correspondingly the thickness and the radius of the quantum dot, and ν_m is the root of the Bessel function J_m. The integrals of interest, $J_{mn} = \int d^3r\ \psi_m^2\psi_n^2$, are equal to: $J_{00} = 2.098$, $J_{11} = 1.552$, and $J_{01} = 1.435$.

It is easy to find all parameters in this approximation. First, let us estimate the magnitude of the spread. To find σ_0 one has to know the volume of the quantum dot. Taking it to be the volume of the cylinder with the thickness 2.5 nm and diameter 25 nm,[1] and using the parameters of InGaAs: $x_0 = 0.5$, lattice constant $a = 0.585$ nm and $(dE_g/dx) = 1.16$ eV (both at $x = 0.5$),[8] we obtain $\sigma_0 = 13$ meV. This value is less than the experimental value of 18.2 meV. It, however, shows that at least a significant part of the spread is caused by the composition fluctuations. There are, of course, some other reasons for spreading. The total spread, however, cannot be less than the calculated value.

Two remaining dimensionless parameters are: $\rho = 0.795$, and $(\sigma_0/\sigma_1) = 1.16$. Though the ratio σ_0/σ_1 is in a reasonable agreement with the experiment, the value of the correlation coefficient ρ is significantly less than the experimental value of 0.94. Note that the dimensionless parameters depend only on the form of the wave functions. Though it is possible to relate the discrepancy in ρ to the unknown shape of the real wave function, there is a more serious reason for this coefficient to be closer to 1.

Among the other causes of spreading of energy levels, which are not taken into account in the presented theory, there are *fluctuations of the shape* of quantum dots. The distortion of the shape of a quantum dot, even when small, cannot be represented as a potential perturbation in the Schrödinger equation. It's effect on the positions and splitting of the energy level E_m can, however, be described by an effective secular matrix δH of the same form as Eq. (6). The only difference is that the matrix elements u and $x + iy$ are not described by the Eqs. (7) any more. Instead, they are determined by the integrals of the derivative of the unperturbed wave function at the boundary of the quantum dot.[9]

Thus, the effect of the shape fluctuations is only in renormalizing the parameters σ_0, σ_m, and ρ. It is important, however, that for the case of pure shape fluctuations, the parameter ρ, defined as a correlation coefficient between u and ϵ_0, is exactly equal to 1. The reason is that in an axially-symmetic quantum dot, the normal derivative of the wave function at the boundary is just a number rather than a function of coordinate. Therefore, there should be an exact relation between u and ϵ_0 *for each particular shape distortion*. It is natural to assume that the effective value of ρ is closer to 1 when both mechanisms are involved, than it is in the case of pure composition fluctuations.

VI. CONCLUSION

In the present paper a simple theory is developed, which allows to describe selective photoluminescence data from an array of quantum dots with random parameters. The theory explains large apparent Stokes-like shift between emission and absorption energies as the average distance between the ground and first excited energy levels in the dots.

It is shown that existence of a random spread of the interlevel distances in the dots causes deviation of the positions of the maxima of the peaks seen in the PL and PLE spectra. Such deviation can make it difficult to determine the properties of the statistical distribution of energy levels in the array. It is suggested how the proper parameters of the statistical distribution may be obtained from the experimental data.

The random shifts and splittings of energy levels caused by a white-noise random potential in the dots are studied. The density of states and mutual level-level distribution function are obtained for the case of axially symmetric quantum dot. The energy-level distribution and the resulting PLE and selectively-excited PL spectra appear to be close to that observed in the experiment

(see Fig. 6). It is shown that the major part of the spread of energies observed in the experiment originates from the random potential caused by the composition fluctuations. It is also suggested that the random fluctuations of the shape of the dots also contribute to the spread.

ACKNOWLEDGMENTS

I am grateful to A. L. Efros for formulating the problem and for numerous illuminating discussions. I would like to thank P. M. Petroff for providing the experimental data prior to the publication. I appreciate important comment by M. E. Raikh and useful discussions with P. M. Petroff, E. I. Rashba, J. M. Worlock, and F. G. Pikus. This work was supported by the Center for Quantized Electronic Structures (QUEST) of UCSB under subagreement KK3017.

---

* e-mail: rr@physics.utah.edu.

[1] S. Fafard, D. Leonard, J. L. Merz, and P. M. Petroff, Appl. Phys. Lett. **65**, 1388, 1994.

[2] J.-Y. Marzin, J.-M. Gérard, A. Izraël, G. Bastard, D. Barrier, Phys. Rev. Lett. **73**, 716, 1994.

[3] M. Grundmann, J. Christen, N. N. Ledentsov, J. Böhrer, D. Bimberg, S. S. Ruvimov, P. Werner, U. Richter, U. Gösele, J. Heydenreich, V. M. Ustinov, A. Yu. Egorov, A. E. Zhukov, P. S. Kop'ev, Zh. I. Alferov, Phys. Rev. Lett. **74**, 4043, 1995.

[4] S. Fafard, R. Leon, D. Leonard, J. L. Merz, P. M. Petroff, Phys. Rev. B **50**, 8086, 1994.

[5] In fact, in order to consider different quantum dots independently it is necessary that average distance between two resonant quantum dots be larger than the wavelength of light. Though average distance between the dots may be smaller than the light wavelength (as it is the case in Ref. 1), the energy levels of close quantum dots coincide seldomly. If, however, the average distance between resonant quantum dots is smaller than the wavelength, the whole array may exhibit some collective-mode effects.

[6] A. Zrenner, L. V. Butov, M. Hagn, G. Abstreiter, G. Böhm, G. Weimann, Phys. Rev. Lett. **72**, 3382, 1994.

[7] A.L. Efros and M.E. Raikh, *Effect of Composition Disorder on the Electronic Properties of Semiconducting Mixed Crystals*, in: *Optical Properties of Mixed Crystals* ed. by R.J. Elliot and I.P. Ipatova, Elsevier, 1988.

[8] Landolt-Börnstein: *Numerical Data and Functional Relationships in Science and Technology*, edited by O. Madelung (Springer-Verlag, Berlin, 1982), Vol. 17, Pts. a and b.

[9] See, e.g., C. C. Johnson, *Field and wave electrodynamics*, McGraw-Hill, N.Y., 1965.

FIG. 1. A schematic diagram of the PLE and selectively-excited PL intensities when interlevel distances in all quantum dots are the same. Each curve is the spectrum taken at fixed excitation energy (PL) or fixed detection energy (PLE), which are denoted by pluses.

FIG. 2. A schematic shape of the intensity as a function of the excitation and detection energies for the system with two excited states. The left "ridge" corresponds to the absorption by the first excited states of the dots. The "PL" and "PLE lines" in the inset are the loci of the positions of the maxima of intensity in the PL and PLE crossections respectively. The dashed lines show the lines of equal intensity. The maxima in a crossection occur at such points where the crossection lines (horizontal and vertical solid lines) are tangential to the lines of equal intensity.

FIG. 3. The function $D_0(z;1)$ (full line), as given by Eq. (9), determines the density of states in the vicinity of the excited level. The approximation by a Gaussian with an effective dispersion (dashed line) is also plotted.

FIG. 4. The two-level mutual distribution function $P(\epsilon_0, \epsilon_1)$ given by Eq. (10) is plotted for fixed $\epsilon_0 = 0$ (the "PLE" curve) and for different fixed ϵ_1 (the set of "PL" curves). The curves are shifted upward arbitrarily to ease the reading. The correlation coefficient is: (a) $\rho = 0.94$ and (b) $\rho = 1$.

FIG. 5. The positions of the PL (crosses) and PLE (pluses) maxima taken from the spectra in Ref. 1 are shown in the combined plot. The resulting crossing lines make clear how the positions of maxima deviate from each other and from the major axis of the first "ridge" (dashed line). The crossection point is the maximum of the ridge. The second set of the PLE maxima is not shown because the corresponding peaks are seen not very clear in the spectra. A constant value of 1290 meV has been subtracted from all energies. The dotted line shows the unit slope, $E_{laser} = E_{detector}$.

FIG. 6. (a) The experimental data from Ref. 1. replotted for comparison. The upper curve is the PLE spectrum obtained with the detection energy marked by an arrow. Pluses above the PLE spectrum show the fixed excitation energies for each of the PL spectra. The curve 9 corresponds to the above-barrier excitation energy. (b) The PLE and selectively-excited PL lineshapes obtained from Eq. (10) with parameters $\rho = 0.94$, $\sigma_0 = \sigma_1 = 19$ meV. Average energy positions of the ground and first excited energy levels are $\overline{E}_0 = 1276$ meV, and $\overline{E}_1 = 1351$ meV.

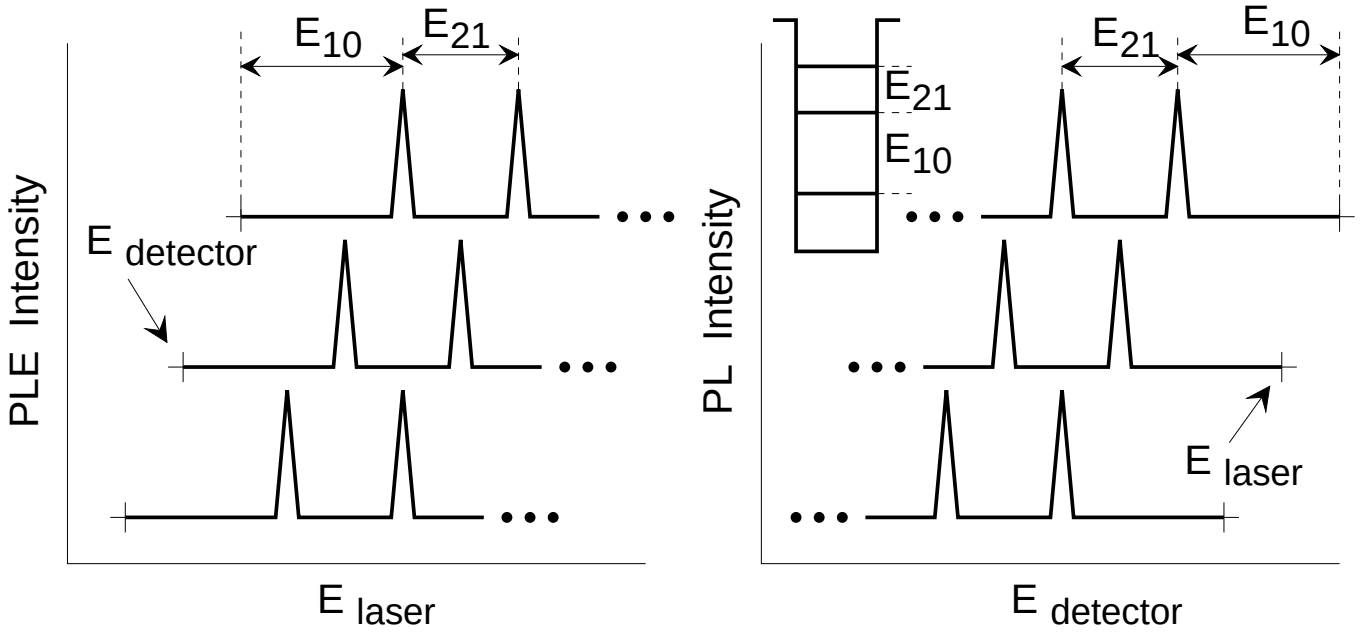
E10
E21
PLE Intensity
E detector
E laser
E21
E10
PL Intensity
E laser
E detector

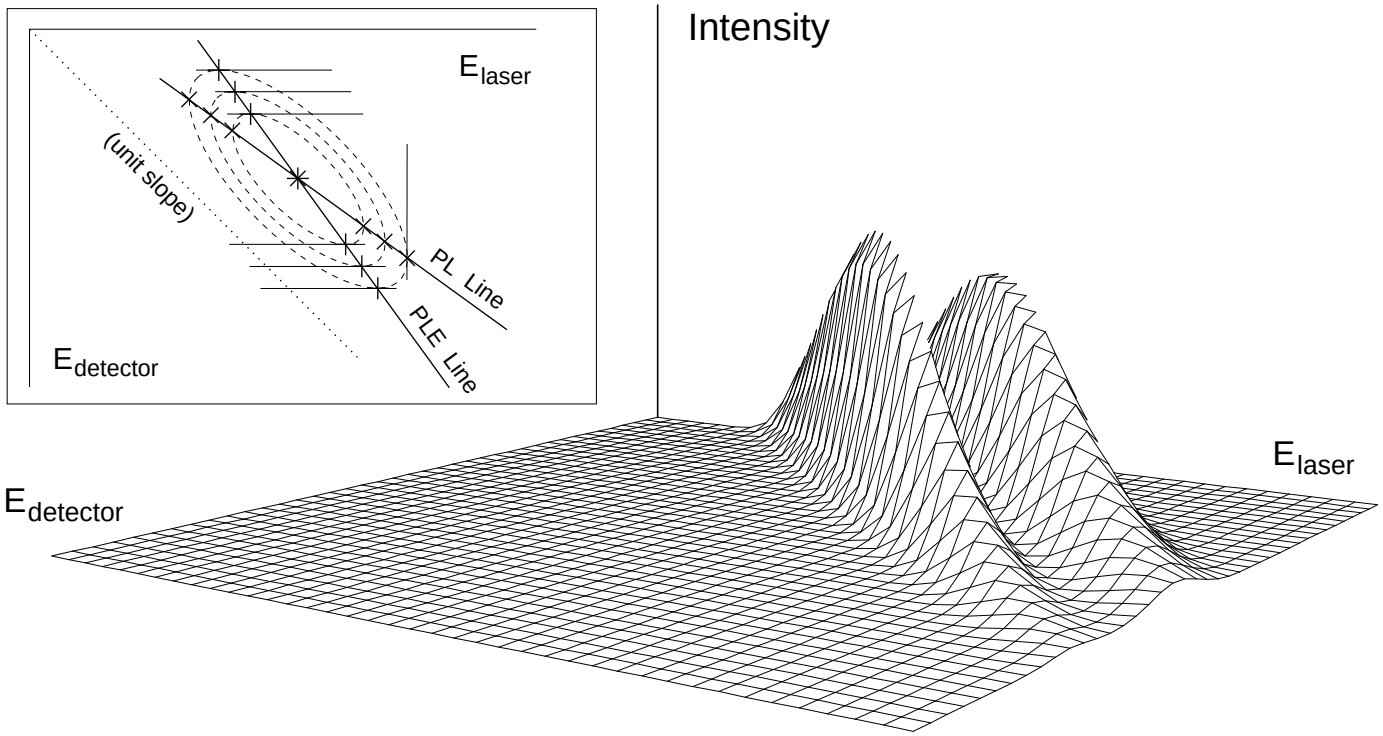
Intensity
E laser
(unit slope)
PL Line
PLE Line
E detector
E laser
E detector

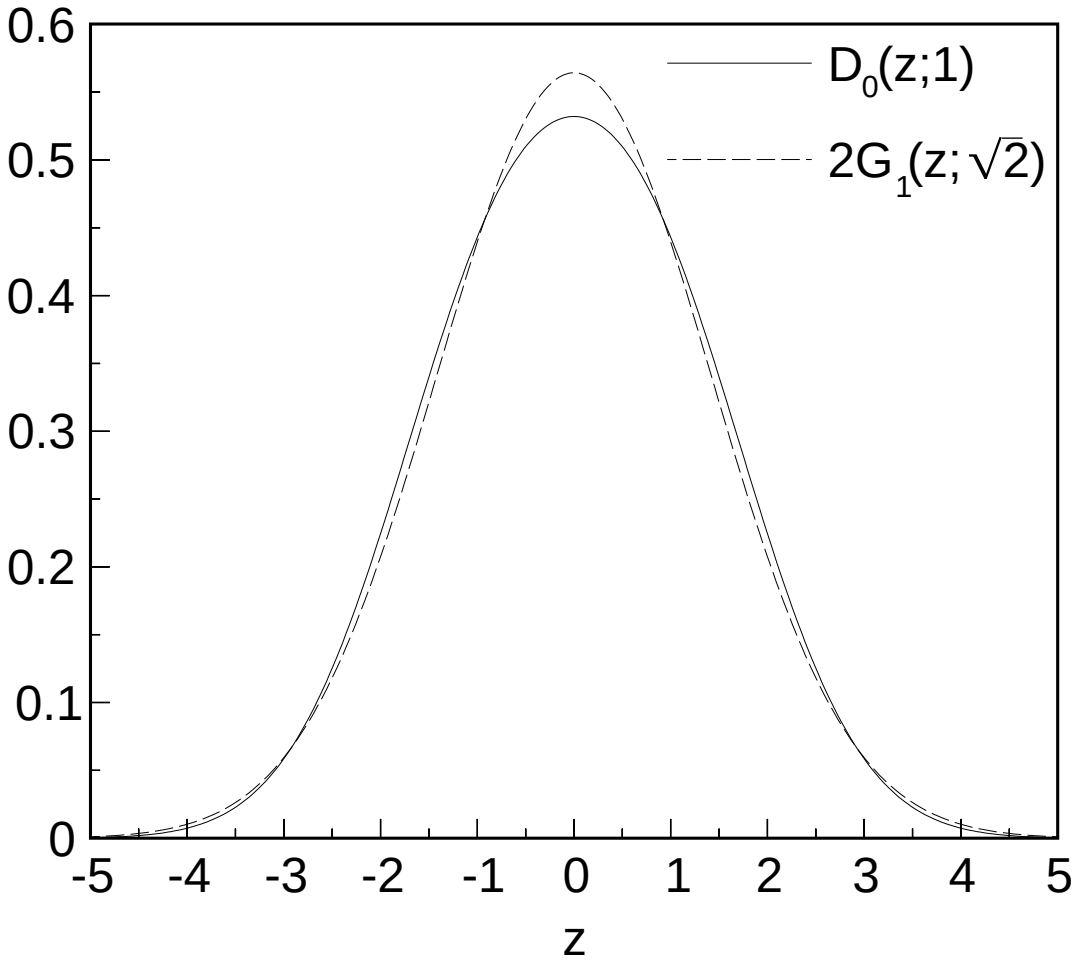
0.6
0.5
0.4
0.3
0.2
0.1
0
-5
-4
-3
-2
-1
0
1
2
3
4
5
z
D0(z;1)
2G1(z;√2)

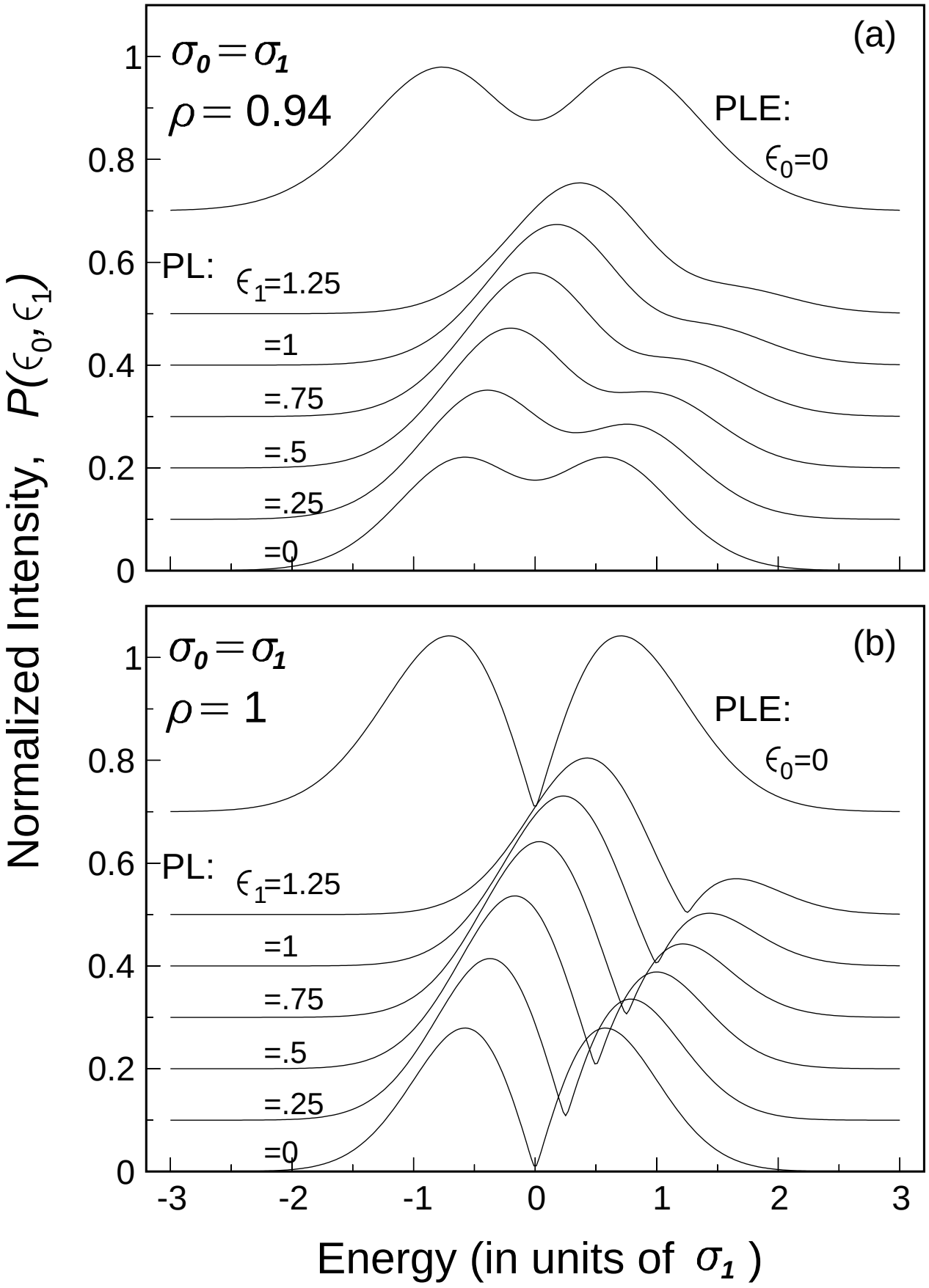
(a)
$\sigma_0 = \sigma_1$
$\rho = 0.94$
PLE:
ϵ_0=0
PL:
ϵ_1=1.25
=1
=.75
=.5
=.25
=0
(b)
$\sigma_0 = \sigma_1$
$\rho = 1$
PLE:
ϵ_0=0
PL:
ϵ_1=1.25
=1
=.75
=.5
=.25
=0
Normalized Intensity, $P(\epsilon_0, \epsilon_1)$
Energy (in units of σ_1)
0
0.2
0.4
0.6
0.8
1
-3
-2
-1
0
1
2
3

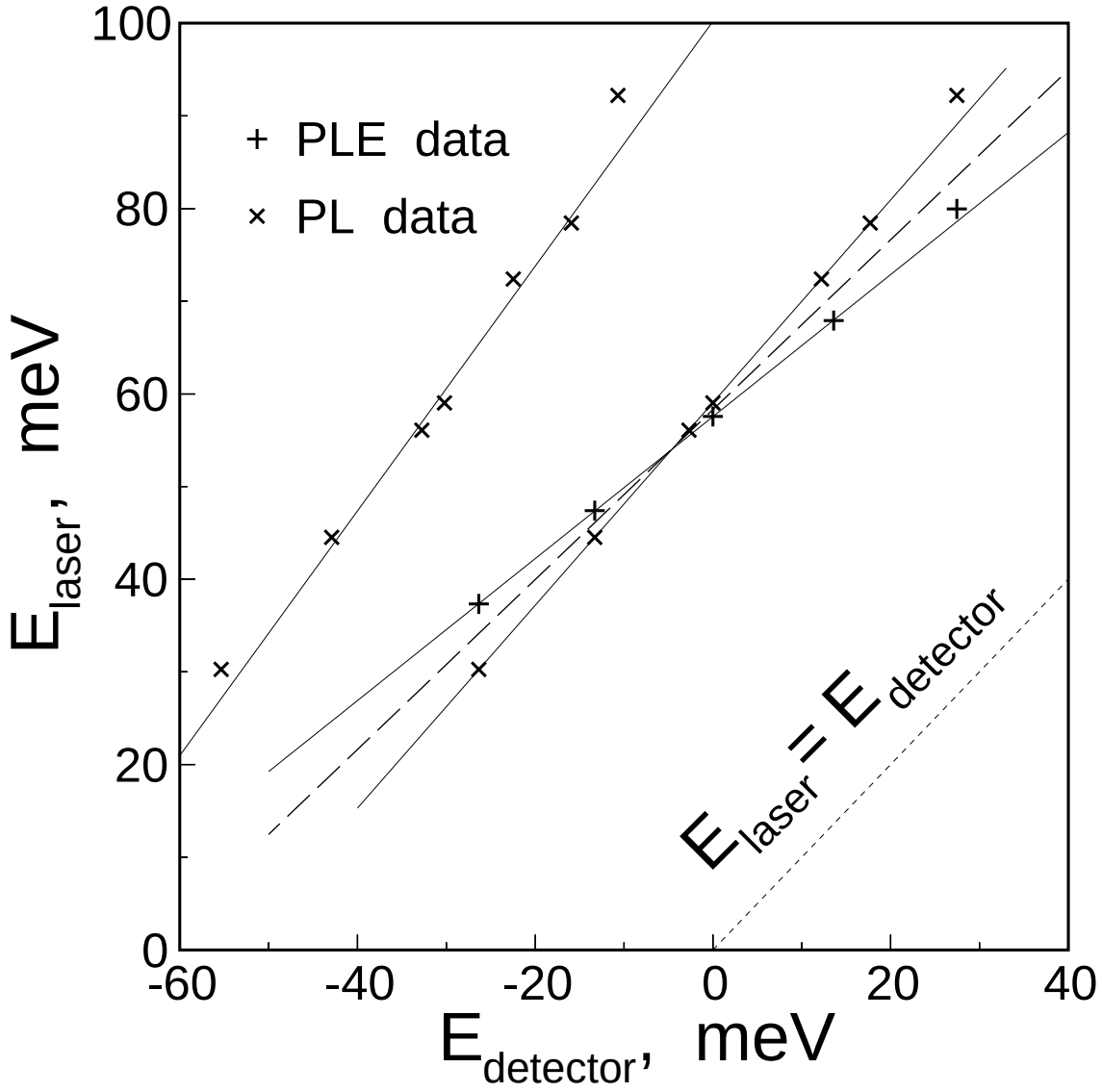
100
80
60
40
20
0
-60
-40
-20
0
20
40
+ PLE data
× PL data
E_laser, meV
E_detector, meV
E_laser = E_detector

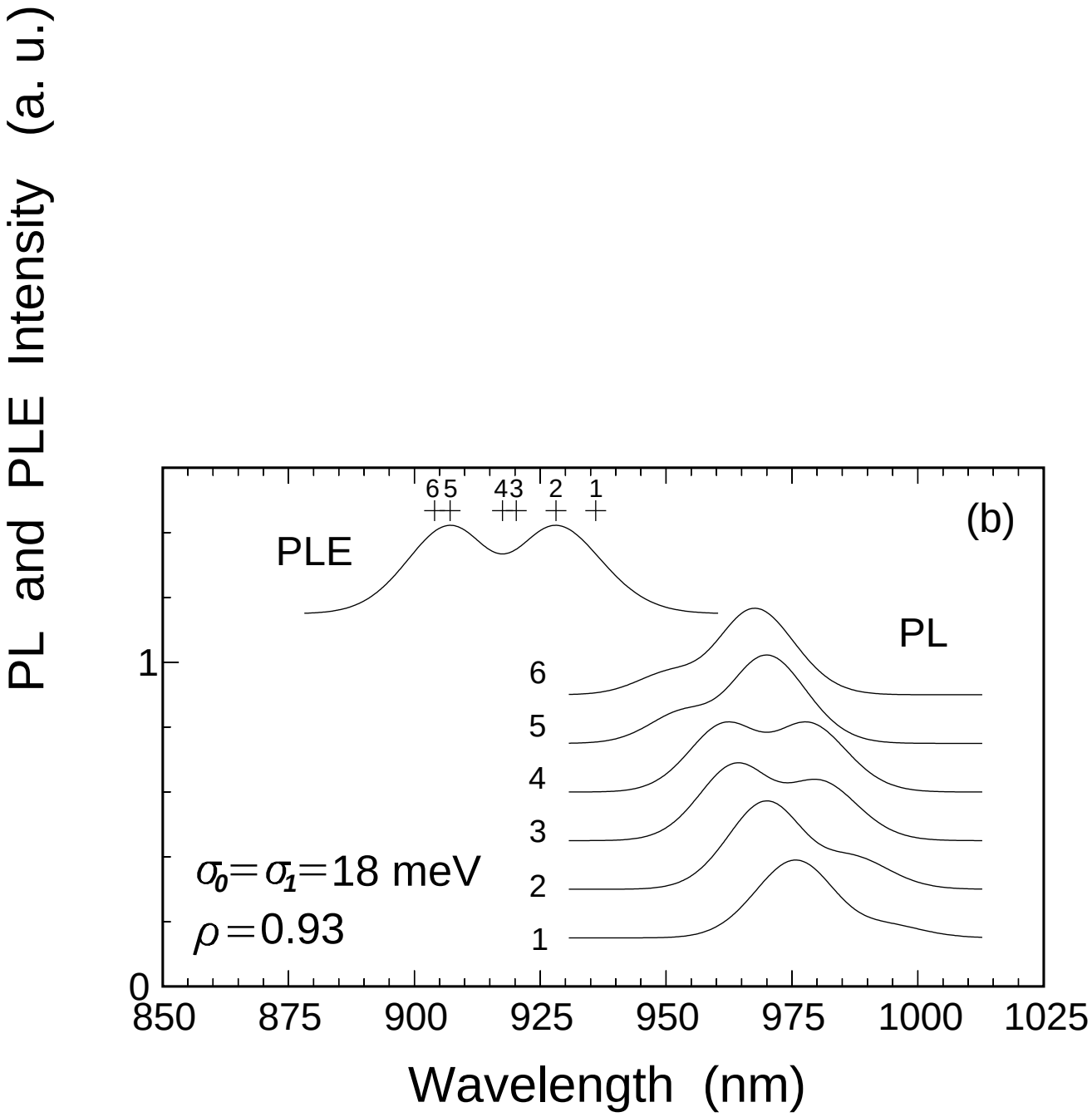
PL and PLE Intensity (a. u.)
6 5
4 3
2
1
(b)
PLE
PL
6
5
4
3
2
1
$\sigma_0 = \sigma_1 = 18$ meV
$\rho = 0.93$
0
1
850
875
900
925
950
975
1000
1025
Wavelength (nm)